Biomass Conversion and Biorefinery
https://doi.org/10.1007/s13399-024-05921-7

ORIGINAL ARTICLE

Fast pyrolysis of the waste lignocellulosic phloem fraction of *Quercus cerris* bark in a twin-screw reactor

Umut Sen[1] · Frederico Gomes Fonseca[2] · Yaxuan Chi[2] · Helena Pereira[1] · Axel Funke[2]

Received: 19 March 2024 / Revised: 20 June 2024 / Accepted: 4 July 2024

Abstract

Tree bark is among the most important lignocellulosic waste materials with high ash, extractive, and lignin contents. These wastes may be valorized through thermochemical methods. The thermochemical conversion of tree bark via fast pyrolysis is usually not economic due to low bio-oil yields and the challenge to valorize biochar in current industrial installations. However, screw-reactor-based fast pyrolysis is a particularly suitable method for producing bio-oils from high ash-containing and heterogeneous lignocellulosic feedstocks. The lower carrier gas requirement and the efficient recovery of biochar make this method economically attractive for the bark of Turkey oak (*Quercus cerris*) which is composed largely of phloem tissues. Here we showed that the phloem of *Q. cerris* can be converted to value-added bio-oils and biochars using the screw reactor without operational problems. The yields of marketable organic liquids and biochars were 32% and 21%, respectively. A process modeling was developed with ASPEN plus software to evaluate the available excess process heat of the fast pyrolysis unit for integration into phloem separation or cork processing units. From an assumed feedstock capacity of 25 MW phloem, 6.8 MW excess heat and 1.5 MW power are supplied in addition to the produced bio-oil. This excess heat can be integrated into bark separation or cork processing operations to save energy and reduce CO_2 emissions.

Keywords Bio-oil · Biochar · Lignocellulose · Biomass · Oak · Phloem

1 Introduction

Tree barks are the exterior protective tissues covering stems, branches, and roots. Bark proportion is highest in branches and lowest in roots, while in the stem, it represents about 10–20% of the wood volume [1, 2]. The amount of bark available as a residual by-product from wood processing is very significant and the world production of bark is estimated to reach as high as 350–400 million m^3 annually [3, 4]. The largest bark-producing industries are sawmills and pulp mills which use industrial round wood as raw material and require debarking as a first operation [5–7]. According to FAO, 1.9 billion m^3 of industrial round wood was produced in 2020, and between 2.5 and 2.9 billion m^3 were predicted for 2050, corresponding to an average increase of 35%. Thus, a much larger production of bark wastes is expected to occur in the near future. A large portion of the produced bark is not utilized or is only combusted at domestic scale, but the chemical richness of bark has triggered attention for its potential valorization, namely as a feedstock for biorefineries.

Highlights
1. Bark fractionation followed by fast pyrolysis was reported for the first time.
2. Phloem can be converted to bio-oils and biochars via fast pyrolysis in screw reactor.
3. Organic liquid and biochar yields were 32% and 21%, respectively.
4. Valorizing excess heat of fast pyrolysis operation was evaluated using process simulation.
5. The integration of fast pyrolysis into cork production was assessed.

✉ Axel Funke
axel.funke@kit.edu

[1] Forest Research Centre, Terra Associated Laboratory, School of Agriculture, University of Lisbon, Tapada da Ajuda, Lisbon 1349-017, Portugal

[2] Institute of Catalysis Research and Technology, Karlsruhe Institute of Technology, Hermann-Von-Helmholtz-Platz 1, 76344 Eggenstein-Leopoldshafen, Germany

Published online: 25 July 2024

In recent years, biorefinery and circular economy concepts have been increasingly applied to waste biomass aiming at reducing CO_2 emission-related environmental pollution and global warming, and also at finding alternative and sustainable fuels to the depleting fossil sources [8]. Thermochemical conversion platforms are among the most successful pathways to valorize biomass as an energy source. Among other processes, fast pyrolysis is a promising method to produce pyrolysis oils (termed bio-oils) at high yields (up to 75%) from lignocellulosic biomass [9]. Although bio-oils are reactive liquids that cannot be used as drop-in fuels, they may be used as industrial boiler fuel or undergo upgrading to produce transportation fuels or chemicals [10].

Fast pyrolysis can be performed with different reactors, and six reactor types have been commonly used including fluidized bed (bubbling and circulating), rotating cone, screw (auger), ablative, and vacuum pyrolysis reactors [10]. The fluidized bed reactors are frequently used since they allow a high heat transfer and fast separation of pyrolysis vapors in easily scalable, well-proven equipment [11, 12]. The fast pyrolysis conditions applied in the different reactor configurations and the biomass particle size and chemical composition affect the yield and composition of pyrolysis products [10]. Among the various reactor concepts available for fast pyrolysis, screw reactor-based fast pyrolysis was shown to be particularly suitable for producing bio-oils from high ash-containing and heterogeneous feed stocks such as wheat straws [13–15]. The lower carrier gas requirement and the possibility to efficiently recover biochar are important advantages of screw reactors compared with, e.g., fluidized bed reactors [16–18].

Cellulose and hemicelluloses are the main contributors to fast pyrolysis bio-oil yield, and therefore wood species with high polysaccharide (cellulose and hemicelluloses) content and low ash content will allow the highest bio-oil yields in pyrolysis [10, 19]. The chemical composition of bark is different from that of wood with lower polysaccharide content and higher extractive and ash contents [2]. This chemical composition results in a lower bio-oil yield, characterized by phase separation and a high ash content [5, 20], as well as operational problems such as agglomeration in fluidized bed reactors [21, 22].

This work studies the fast pyrolysis of a residual bark fraction in a screw reactor using the bark of Turkey oak (*Quercus cerris*) as the case study feedstock. *Q. cerris* has a cork-rich bark that upon fractionation yields about 35% of cork and 65% of a phloem fraction [23]. The cork fraction is valued for use in agglomerated cork products since *Q. cerris* cork has a cellular structure and chemical composition similar to those of the commercial *Q. suber* cork. The phloem fraction is presently not utilized but its valorization is required for an economically integrated use of the bark. The chemical lignocellulosic nature of phloem suggests that it may be converted to value-added chemicals or biochars through extraction, mild pyrolysis, or slow pyrolysis [24]. The objective of this study is to investigate the fast pyrolysis properties of *Quercus cerris* phloem regarding physical, chemical, and fuel properties, and characterize the pyrolysis bio-oils and biochars obtained in fast pyrolysis experiments. Mass, energy, and carbon balances are evaluated to investigate how fast pyrolysis can be integrated in a cork production facility.

2 Materials and methods

2.1 Material

Quercus cerris barks were collected from the stumps of recently harvested mature trees from the Amanos mountains (Hatay, south of Turkey). The bark samples were ground into coarse fractions with a hammer mill on site. After shipment to the laboratory, they were fractionated in a pilot scale equipment, sieved, and screened into pure cork fractions and waste phloem fractions via a granulometric and density separation [23]. The waste phloem fractions used in this study contained a small proportion of residual cork. The average particle size was 180–250 µm although it also contained larger residual cork particles.

2.2 Methods

The experiments used previously described waste *Quercus cerris* phloem granules. All experiments were performed in duplicate.

2.2.1 Characterization of physical and fuel properties of phloem and biochar

Moisture content of raw phloem and phloem chars was determined according to DIN EN 14774–3: (ISO 18134) standard by drying at 105 °C until constant weight. Ash content of raw phloem and phloem chars was determined according to DIN EN 14775b (ISO 18122) standard using three different final temperatures of 550 °C, 815 °C, and 1000 °C. The bulk density of the phloem was calculated by placing the phloem granules into a calibrated cylinder and measuring the weight occupying the volume without using an external compacting force. The tapped density was calculated by calculating the phloem mass occupying the volume after mechanical tapping of the granules until achieving a constant volume. The compressibility index (CI) and Hausner ratio (HR) were calculated using the following equations after calculating the bulk (ρ_{bulk}) and tapped (ρ_{tapped}) densities:

$$CI = 100x(\frac{\rho_{tapped} - \rho_{bulk}}{\rho_{tapped}}) \quad (1)$$

$$HR = (\frac{\rho_{tapped}}{\rho_{bulk}}) \quad (2)$$

The higher heating value (HHV) of phloem was determined following DIN EN 14918 standard, while the higher heating value of phloem chars was calculated according to DIN 51900–2/3 standard using a bomb calorimeter. Inorganic elemental analysis of raw phloem was carried out with the ICP-AES technique. Organic elemental analysis (CHNO) of phloem was carried out according to DIN EN 15104 standard, while organic elemental analysis of phloem biochars was carried out following DIN 51732 standard.

The thermogravimetric analysis (TGA) of phloem was conducted with TA Instruments SDT 2960 simultaneous DSC-TGA analyzer using alumina pans under air or nitrogen flow rates between 20 and 50 mL min^{-1}. For the thermogravimetric analyses, a linear heating program with a heating rate of 10 °C min^{-1} was applied with approximately 5 mg phloem samples.

2.2.2 Chemical summative composition

Chemical summative analyses of phloem included determinations of ash, extractives soluble in dichloromethane, ethanol, and water, suberin, Klason lignin, and acid-soluble lignin. Ash content was determined according to TAPPI Standard T 15 os-58 using 2.0 g of phloem that was incinerated at 500 °C overnight and the residue weighed. Extractive content was determined by successive Soxhlet extractions according to TAPPI Standards (T204 om-88 and T207 om-93) with dichloromethane (DCM), ethanol, and water during 6 h, 18 h, and 18 h extraction time for each solvent, respectively.

The suberin content (contained in the residual cork present in the fraction) was determined from depolymerization using methanolysis on the extractive-free material [25]. Approximately 1.5 g extractive-free sample was refluxed with 100 mL of a 3% methanolic solution of $NaOCH_3$ in CH_3OH for 3 h, filtrated, and washed with methanol. The residue was refluxed with 100 mL CH_3OH for 15 min and filtrated again. The combined filtrates were acidified to pH 6 with 2 M H_2SO_4 and evaporated to dryness. The residues were suspended in 50 mL water and the alcoholysis products were recovered with dichloromethane in three liquid–liquid extractions, each with 50 mL DCM. The combined extracts were dried over anhydrous Na_2SO_4, and the solvent was evaporated to dryness.

Klason and acid-soluble lignin contents were determined according to TAPPI T 222 om-88 and TAPPI UM 250 standards on the extracted and desuberinized material. Sulfuric acid (72%, 3.0 mL) was added to 0.35 g of the material, and the mixture was placed in a water bath at 30 °C for 1 h after which the sample was diluted to a concentration of 4% H2SO4 and hydrolyzed for 1 h at 120 °C [26]. The sample was vacuum-filtered through a crucible and washed with boiling distilled water. The polysaccharide content of the samples was calculated by mass difference.

2.2.3 Pilot-scale fast pyrolysis

Pilot scale fast pyrolysis experiments were carried out at the fast pyrolysis unit of Karlsruhe Institute of Technology (KIT). The experimental equipment and procedure is described in detail elsewhere, including a video to experience the scale of the unit (Fig. 1) [15]. A twin-screw reactor with a reactor length of 1.5 m and a screw diameter of 4 cm was used to pyrolyze ground *Q. cerris* phloem samples. The operational conditions were as follows: biomass feed rate of 4.6 kg h^{-1}; reactor outlet temperature 500 °C; vapor residence time less than 2 s; inert gas nitrogen; and mass ratio of biomass to heat carrier (steel beads) 1:100. After the reactor, hot pyrolysis vapors passed two cyclones in series for particle removal (biochar). The hot vapors were then quenched by recirculated condensate to a temperature of around 90 °C to yield an organic-rich condensate. An electrostatic precipitator was applied to capture aerosols after quenching at the same temperature; this fraction was collected together with the organic-rich condensate. The organic-rich condensate is comparable to "common" fast pyrolysis bio-oil but condensed at slightly higher temperatures to prevent phase separation which typically occurs for ash-rich feedstock. A second liquid fraction, the aqueous condensate, was recovered at temperatures around 20 °C. The remaining uncondensed gases were measured with an online GC and vented. Mass balances were determined by weighing the feedstock and products over the length of one run which typically lasts around 4 h.

Since start up material is required to operate the two condensation loops (ethylene glycol in the first and water in the second) and there is a limited duration of one experiment, the produced condensates contain > 50% of this start-up material after the experiment. To characterize condensates without this starting material, a sampling train was installed that extracts hot pyrolysis gas during steady-state operation just before entering the first quench. This sampling train resembles the main condensation, i.e., two stages at 90 °C/20 °C with an electrostatic precipitator for the first condensation step, with the difference that indirect heat exchangers are

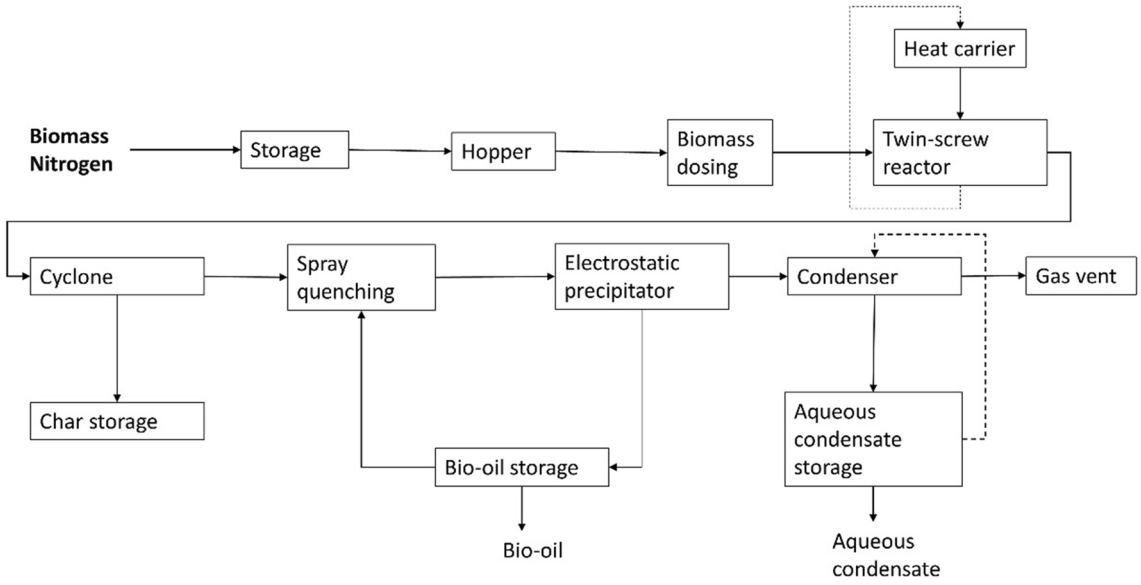

Fig. 1 Block flow diagram of fast pyrolysis. Adapted from [15]

used instead of quenching. Moreover, a ceramic filter was installed at the inlet of this sampling train to minimize the solids content of the produced condensates. The samples obtained in this manner are sent for GC analyses.

The fast pyrolysis experiment was conducted in duplicate and a reasonable reproducibility was achieved in terms of mass balances. A total of > 30 kg phloem was pyrolyzed in these two runs.

2.2.4 Composition of fast pyrolysis bio-oil

The water content of bio-oils was determined by volumetric Karl Fischer titration with Hydranal Composite V. The elemental composition of carbon, hydrogen, and nitrogen was measured with a Vario EL III analyzer using the complete oxidation method. The oxygen content was determined by difference. GC-FID/MS analyses followed a method specifically developed for pyrolysis oils; details are published elsewhere [27].

2.2.5 Process modeling

The process is dimensioned at 25 MW feedstock capacity of undried biomass (Fig. 2). The feedstock biomass is not represented in the model; instead, the pyrolysis products are the starting point for which the mass flows and compositions were determined based on experimental results. This setup was decided because the focus of the process simulation is on the evaluation of available energy from by-products (and not on modeling pyrolysis reaction itself).

The organic-rich condensate from the first condensation stage, i.e., fast pyrolysis bio-oil, is not modeled in more detail since it is recovered as the main product in all the simulated cases. The aqueous condensate from the second condensation stage is simulated as a mixture of water and acetic acid to represent its organic content. This is a strong simplification even though acetic acid is the main organic compound typically observed in the aqueous condensate but its impact on the intended energetic evaluation is very low due to the amount and nature of the aqueous condensate. Uncondensed gases are represented as a mixture of CO_2, CO, H_2, CH_4, and C_3H_8 as representative of C2 + species. The coke is modeled as a nonconventional material, and the strategy for its decomposition is detailed in Supplemental Table 3.

Pyrolysis by-products are either separated or fed into a furnace depending on the simulated case. The furnace is operated with an excess oxygen of 10%. Before using the generated heat in the flue gas from combustion for a heat recovery steam generator, heat demand for the enthalpy change resulting from the coke decomposition block is covered via a virtual heat exchanger (in reality, this enthalpy change would occur during combustion). Also, heat demand for pyrolysis is extracted at this stage with a heat exchanger set to a specified heat demand. The residual heat in the flue gas leaving the heat recovery steam generator is used to preheat incoming combustion air before it enters the furnace.

The combined heat and power generation (CHP) is implemented as a steam cycle without material and energy losses including a steam generator, steam turbine, condenser, and pump for recirculation.

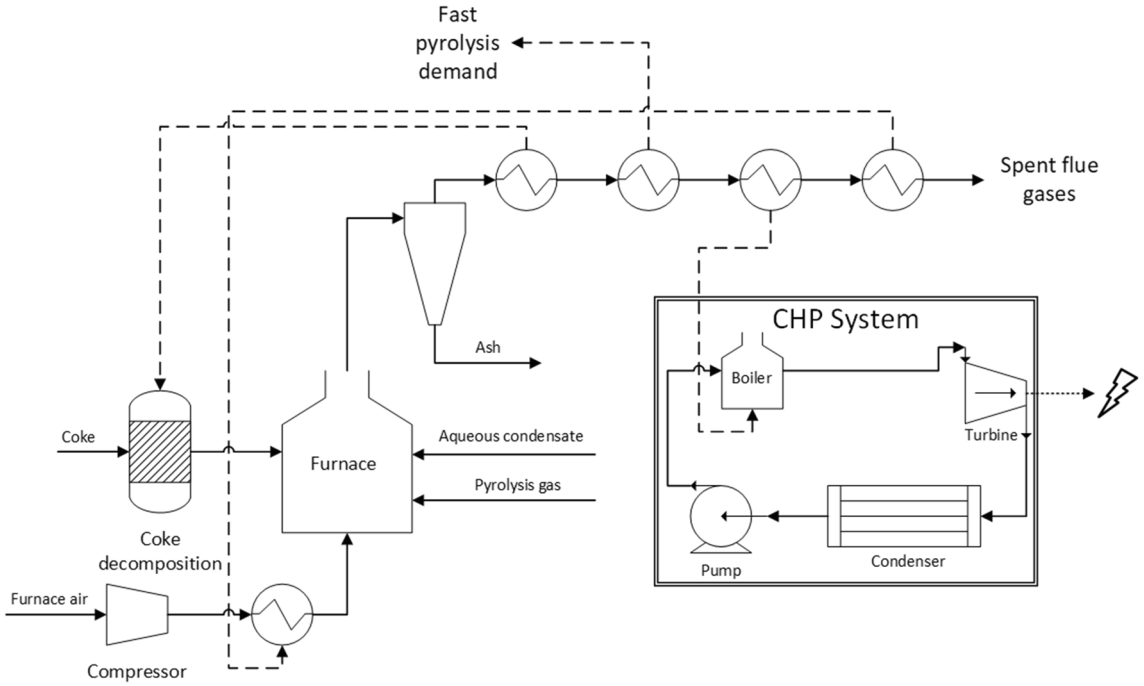

Fig. 2 Scheme of the model for conversion of pyrolysis side products into electrical power using CHP. Solid lines represent material streams, dashed lines represent heat streams, and dotted lines represent work streams

3 Results and discussion

3.1 Physical and chemical properties of phloem and biochars

The physical properties relevant to fast pyrolysis include moisture, ash, and volatile contents as well as density, flow properties, and calorific content (Table 1). Moisture content affects the process economy, product yield, and composition of pyrolysis oil. Whereupon the biomass has a high moisture content, a higher amount of energy is required to supply in pyrolysis, reducing the process efficiency. The moisture of biomass also ends up in condensates and affects the yield and composition of bio-oil. A high moisture content in the condensate may also result in a phase separation [28].

Table 1 Physical properties of *Quercus cerris* phloem and biochar

Property	Phloem	Biochar	Unit
Moisture content	10.3 ± 0.1	3.5 ± 0.6	%
Ash (550 °C)	10.0 ± 0.1	32.0 ± 3.4	%
Ash (815 °C)	6.2 ± 0.1	20.6 ± 1.7	%
Ash (1000 °C)	6.2 ± 0.1	20.2 ± 1.9	%
Volatile content	71.0 ± 0.1	30.5 ± 6.6	%
Bulk density	500 ± 14	-	kg m^{-3}
Tapped density	575 ± 7	-	kg m^{-3}
Compressibility index	13	-	%
Hausner ratio	1.15	-	-
HHV	16.6	20.1 ± 1.3	MJ kg^{-1}

The moisture content of *Q. cerris* phloem was approximately 10% which is a common range of air dry biomass [29] (Table 1). The ash content of phloem was high and was between 10 and 12% where approximately 40% of the ash was lost at high temperatures over 815 °C (Tables 1 and 2). The high ash content (> 2.5%) of phloem may lead to secondary catalytic reactions increasing the water content in bio-oil as well as leading to ash concentration in bio-oil [28].

The volatile content of phloem was 71% and the bulk density was 500 kg m^{-3}. The density of phloem particles increased by 15% after tapping. The flow properties of phloem particles were satisfactory with a compressibility index lower than (15%) and Hausner ratio close to 1. The higher heating value of phloem was 16.6 MJ kg^{-1} (Table 1).

The summative chemical composition of *Q. cerris* phloem is shown in Table 2. The overall chemical composition is a typical lignocellulosic material with lignin and polysaccharides making up approximately 77% of the dry weight. The extractive content was low (4.6%) and suberin was present in a small amount (3.0%) resulting from the presence of some cork granules in the waste phloem material. A distinguishing feature of phloem was its high ash content which is similar to agricultural residues such as wheat

Table 2 Summative chemical composition of *Quercus cerris* phloem (% dry weight)

Component	% dry weight
Ash	12.34 ± 0.02
DCM extractives	0.40 ± 0.00
EtOH extractives	0.43 ± 0.03
H_2O extractives	3.73 ± 0.35
Total extractives	4.57 ± 0.38
Suberin	2.95 ± 0.26
Klason lignin	32.76 ± 1.23
Soluble lignin	3.17 ± 0.11
Total lignin	35.93 ± 1.60
Polysaccharides	44.21 ± 2.00
Ash components	% of ash
Ca	80.42 ± 11.36
Si	9.16 ± 11.17
K	4.06 ± 0.42
Fe	2.86 ± 0.80
Al	1.30 ± 0.01
Mg	1.05 ± 0.06
S	0.61 ± 0.09
P	0.30 ± 0.03
Na	0.22 ± 0.01

straw or rice husk [15, 30]. Calcium, silicon, potassium, and iron were the main components of phloem ash.

The organic elemental composition of *Q. cerris* phloem is shown in Table 3. Fast pyrolysis increased the carbon content in biochar by approximately 30%, hydrogen content was reduced by approximately 50%, and oxygen content was reduced by 23%.

The thermal degradation of *Q. cerris* phloem is shown in Fig. 3. A total of four different processes are observed at temperatures of approximately 279 °C, 365 °C, 502 °C, and 678 °C which correspond to the degradation of hemicelluloses, cellulose, char, and inorganics. The thermal degradation of phloem under combustion conditions occurred at temperatures approximately 30 °C lower than pyrolysis except for hemicellulose degradation which occurred under similar temperatures. The phloem was reactive until 670 °C under oxidative conditions, and its pyrolysis resulted in approximately 20% char yield.

3.2 Mass and carbon yields of fast pyrolysis

Quercus cerris phloem could be converted in the fast pyrolysis unit without observing any problems. The results of mass balances are summarized in Fig. 4. The observed deficit is reasonable for a fast pyrolysis unit in that scale and can be largely explained by volatiles that escape the second condenser and are not detected by the GC/MS (both organics and water). The organic liquid yield, i.e., combined condensate yield excluding water on a dry feedstock basis, was 32.3 wt.%. Being an ash-rich feedstock, fast pyrolysis bio-oil (FPBO) yields from *Quercus cerris* phloem were expected to be comparably low (see Table 4). The organic liquid yield is in line with trends observed in the literature that investigates the influence of ash content on organic liquid yield [31]. Specifically, it corresponds well to the empiric correlation derived from the same experimental setup, which would predict an organic liquid yield of only 27 wt.% for a feedstock ash content of 10 wt.% [32]. This indicates comparably good bio-oil potential for the high ash content contained in *Quercus cerris* phloem.

Table 3 Elemental compositions and atomic ratios of *Quercus cerris* phloem and biochar (% dry weight)

Element (%)	Phloem	Biochar
C	45.6	59.4
H	5.6	2.6
N	0.3	0.7
*O	48.5	37.3
H/C	1.45	0.52
O/C	0.55	0.90

*Calculated by difference (%O = 100 − %C − %H − %N − %Ash)

3.3 Characterization of fast pyrolysis bio-oil

The composition of fast pyrolysis bio-oil of *Q. cerris* phloem is shown in Fig. 5 and Online Resource 1. Aromatic compounds were the major components of bio-oil with lignin-derived guaiacols, syringols, and simple phenols being the principal compounds. Bio-oil also contained a significant fraction of polysaccharide-derived furans as well as polysaccharide-derived nonaromatic ketones; however, their amount is much lower than typically observed [34]. While the amount of levoglucosan is comparable to results observed elsewhere, almost no hydroxyl acetaldehyde is observed despite being a significant fraction of fast pyrolysis bio-oil [35]. This is a direct effect of the chosen condensation temperature, which is higher compared to typically applied temperatures (90 °C vs 70–60 °C). Noteworthy is also the relatively high content of low molecular weight lignin-derived compounds, specifically phenols, guaiacols, and syringols, whose occurrence is directly related to feedstock composition. Moreover, the amount of undetected compounds by the applied GC method is surprisingly high, which hints at the existence of a very high fraction of high molecular weight compounds, i.e., oligomers. This might be a combined effect of feedstock composition and the high ash content of the feedstock.

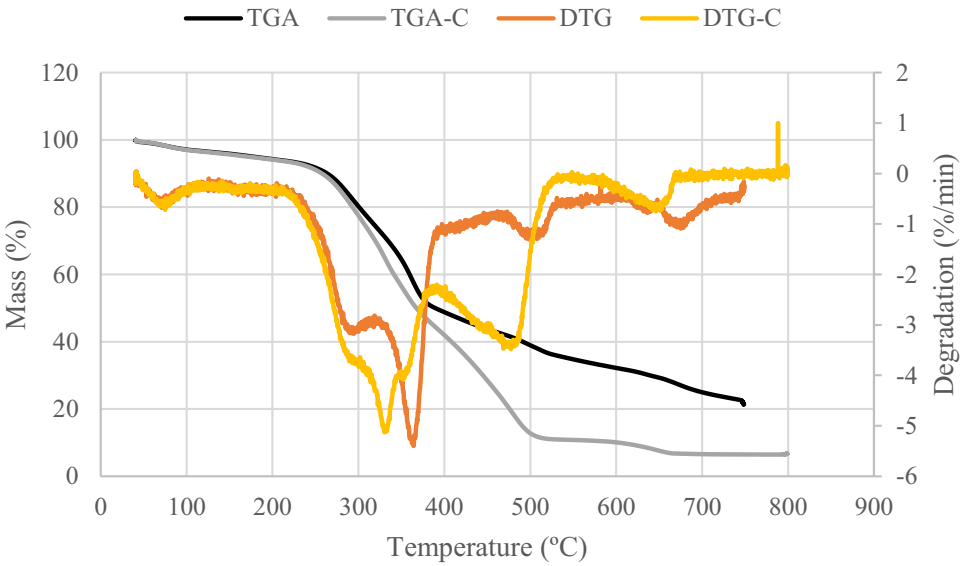

Fig. 3 Thermal degradation of *Quercus cerris* phloem. Heating rate: 10 °C/min. Nitrogen flow rate: 55 ml/min, Air flow rate: 48 ml/min. C: combustion (degradation under airflow)

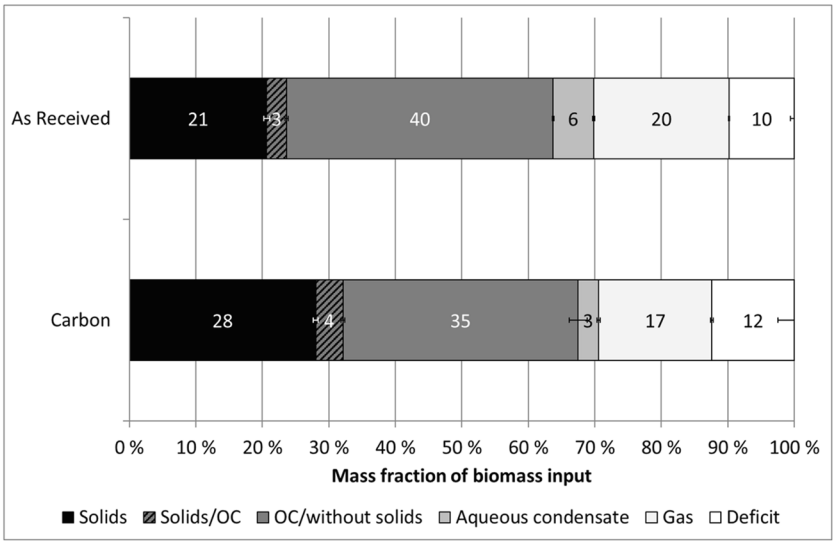

Fig. 4 Total mass (as received basis) and carbon yields after fast pyrolysis of *Quercus cerris* phloem. OC refers to "organic-rich condensate." Error bars indicate maximum deviations from the mean of the duplicate runs

3.4 Process modeling

Cork processing mills in Portugal produce approximately between 100 and 187 thousand tons of cork products per year. The cork production results in 25–30% cork waste powder which corresponds to approximately 17 and 45 thousand tons of waste which is valorized for material and energy production [36]. The energy is primarily used to cover the heat demand of the cork processing mills on site. The leading cork-producing company in Portugal uses a co-generation unit to produce 1,075 TJ energy per year which corresponds to an approximate reduction of 71,000 tons of CO_2 emissions, according to the latest sustainability report of the company in 2020 [37].

Incorporating the phloem separation process into the cork processing unit operations will raise the energy consumption of a cork processing facility. Nonetheless, the precise energy usage associated with this supplementary separation step remains largely unspecified. This process includes the milling of bark chunks (*i*) followed by pneumatic transport (*ii*) and a density separation (*iii*) of waste phloem and high- and low-density cork fractions. It follows that additional electric power is primarily needed.

Similar to cork waste powder, phloem could be burned directly on-site to increase the capacity of an existing co-generation facility. Given the fact that only a fraction of cork waste powder is combusted after added value (i.e., material) uses have been exploited and that the separated phloem amounts to twice as much weight as the cork fraction, it follows that the energy available from on-site waste combustion will increase by at least on order of magnitude when changing the feedstock to *Quercus cerris*. With an approximate LHV of 15 MJ/kg phloem, an additional

Table 4 Comparison of ash, biochar, and organic liquid yields of different feedstocks and different reactors

Feedstock	Ash (%)	Char (%)	Organic liquid yield (%)	Reactor	Reference
Q. cerris phloem	10	21	32	Twin-screw	This study
Wheat straw	9.2	19	35		[15]
Miscanthus	2.7	12	46		[15]
Scrap wood	1.5	13	50		[15]
Wheat straw	4.9	28	21	Fluidized bed	[33]
Switch grass	5.7	20	45		
Miscanthus	4.5	31	41		
Willow	3.0	20	44		
Beech wood	1.0	14	55		
Barley straw	5.8	-	36	Fluidized bed	[31]
Rape straw	6.1	-	45		
Forest residue	3.8	-	46		
Eucalyptus wood	0.4	-	60		
Pine wood	0.1	-	62		

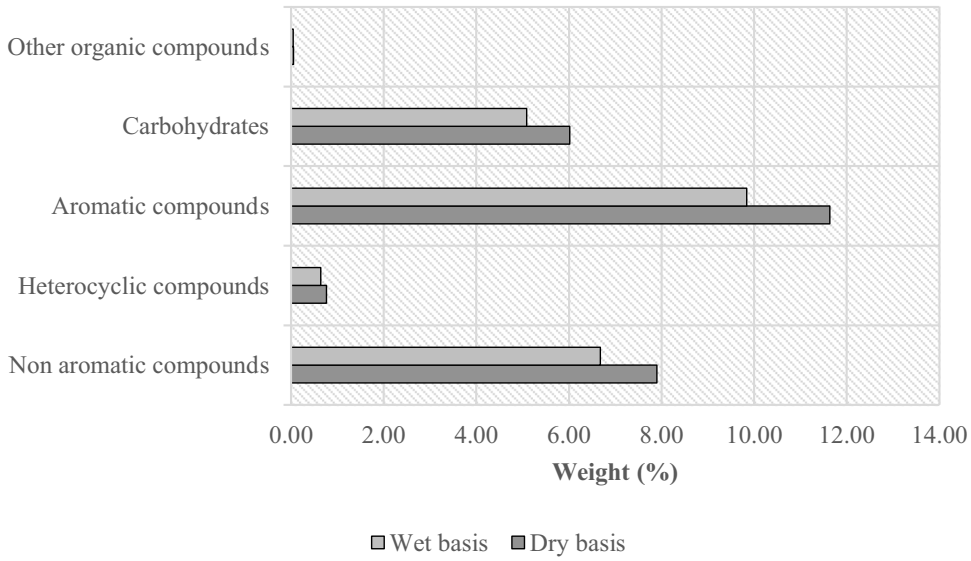

Fig. 5 Main compound groups of fast pyrolysis bio-oil of *Quercus cerris* phloem

heat of 30 GJ/ton cork can be supplied (excluding cork waste powder combustion). This results in a tremendous increase in available energy which may be either beneficial or superfluous depending on site-specific conditions.

The state-of-the-art industrial fast pyrolysis is capable of producing a liquid biofuel and at the same time utilizing surplus waste heat for combined heat and power production. This can be made through the combustion of the by-produced solids and uncondensed gases, either by an integrated steam cycle (as, e.g., realized in the Empyro facility) or by adding a fast pyrolysis unit to an existing power plant (as, e.g., realized in the Joensuu facility) [38]. Application of fast pyrolysis to residual phloem will consequently add a level of flexibility to a cork processing mill while reducing the available heat that needs to be utilized on-site.

Table 5 Mass and heat balances from process simulation

	Phloem	Bio-oil	Biochar	Uncondensed gas
Mass flow (ton h^{-1})	4.6	1.9	1.1	1.6
Heat (MW)	25.0	10.6	7.0	7.6

Results from the process model based on the experiments presented in this study are summarized in Table 5 and Online Resources 2–5. For the small-scale steam cycle that was considered for integration in the fast pyrolysis unit, 6.8 MW heat and 1.5 MW power can be supplied through the combustion of the by-products from fast pyrolysis in addition to supplying heat to the fast pyrolysis process. Alternatively, biochar could

be recovered separately, reducing the heat from the steam cycle to 1.2 MW and the power output to 0.3 MW. In such a case, it would be unlikely that an additional steam cycle is economically feasible to be integrated into the fast pyrolysis unit; however, economics becomes different if the fast pyrolysis unit is attached to an existing biomass combustion facility instead. These two alternatives (including and excluding biochar combustion) result in additional heat generated from the combined heat and power cycle of as detailed above.

4 Conclusions

Fast pyrolysis of waste *Q. cerris* phloem was performed in a twin-screw fast pyrolysis reactor. The physical and chemical properties of raw phloem, phloem biochars, and phloem bio-oils were analyzed. A process modeling was developed with Aspen Plus software to evaluate the available excess process heat of the fast pyrolysis unit for integration into phloem separation or cork processing units.

It was found that the waste fraction of *Q. cerris* phloem can be converted to bio-oils and biochars in a twin-screw reactor without any operational problems. The yield of organic liquids was 32% and biochar yield was 21%, which is in line with the high ash content of the feedstock. The excess heat available from fast pyrolysis processes can be integrated into bark separation or cork processing operations to save energy and reduce CO_2 emissions. It was found that the high amount of by-product (i.e., phloem) from bark separation increases the available heat from onsite combustion by one order of magnitude compared to a traditional cork processing unit. As alternative to this combustion, fast pyrolysis offers the possibility to produce marketable products in addition to excess heat, which might be a favorable option depending on the specific circumstances of cork processing units.

Supplementary Information The online version contains supplementary material available at https://doi.org/10.1007/s13399-024-05921-7.

Acknowledgements The authors thank Joaquina Silva for chemical analysis of phloem. The authors thank Melany Frank, Pia Griesheimer, Petra Janke, Jessica Maier, Daniel Richter, and Norbert Sickinger for support with experiments and analyses.

Author contribution Umut Sen: concept and writing of the original draft. Frederico Fonseca: development of the process model. Yaxuan Chi: development of the process model. Helena Pereira: review and editing. Axel Funke: concept and writing of the original draft.

Funding Open Access funding enabled and organized by Projekt DEAL. This work has been supported by FCT – Fundação para a Ciência e a Tecnologia within the R&D Unit Forest Research Centre, CEF (https://doi.org/10.54499/UIDB/00239/2020andhttps://doi.org/10.54499/UIDP/00239/2020). U. Sen acknowledges support from FCT through a research contract (DL 57/2016). The research visit and fast pyrolysis experiments were funded by the European Union's Horizon 2020's research and innovation program under grant agreement number 731101.

Declarations

Competing interests The authors declare no competing interests.

References

1. Harkin JM, Rowe JW (1971) Bark and its possible uses. U.S. Department of Agriculture, Forest Service and Forest Product Laboratory, Madison, Wisconsin (Research Note FPL; 091), p 56
2. Fengel D, Wegener G (1984) Wood: chemistry, ultrastructure, reactions. Walter de Gruyter, Berlin/New York
3. Pasztory Z, Mohácsiné IR, Gorbacheva G, Börcsök Z (2016) The utilization of tree bark. BioResources 11:7859–7888. https://doi.org/10.15376/biores.11.3.Pasztory
4. Şen AU, Pereira H (2021) State-of-the-art char production with a focus on bark feedstocks: processes, design, and applications. Processes 9(1):87. https://doi.org/10.3390/pr9010087
5. Mohan D, Pittman CU Jr, Steele PH (2006) Pyrolysis of wood/biomass for bio-oil: a critical review. Energy Fuels 20:848–889. https://doi.org/10.1021/ef0502397
6. Pietarinen SP, Willför SM, Ahotupa MO et al (2006) Knotwood and bark extracts: strong antioxidants from waste materials. J Wood Sci 52:436–444. https://doi.org/10.1007/s10086-005-0780-1
7. Kwan I, Huang T, Ek M et al (2022) Bark from Nordic tree species–a sustainable source for amphiphilic polymers and surfactants. Nord Pulp Pap Res J 37(4):66–575. https://doi.org/10.1515/npprj-2022-0003
8. Kamm B, Kamm M, Gruber PR, Kromus S (2005) Biorefinery systems–an overview. In: Kamm B, Gruber PR, Kamm M (eds) Biorefineries-Industrial Process and Products. WILEY-VCH, Weinheim. https://doi.org/10.1002/9783527619849.ch1
9. Bridgwater AV, Toft AJ, Brammer JG (2002) A techno-economic comparison of power production by biomass fast pyrolysis with gasification and combustion. Renew Sustain Energy Rev 6:181–246. https://doi.org/10.1016/S1364-0321(01)00010-7
10. Venderbosch RH, Prins W (2010) Fast pyrolysis technology development. Biofuels, Bioprod biorefining 4:178–208. https://doi.org/10.1002/bbb.205
11. Meier D, Faix O (1999) State of the art of applied fast pyrolysis of lignocellulosic materials—a review. Bioresour Technol 68:71–77. https://doi.org/10.1016/S0960-8524(98)00086-8
12. Amutio M, Lopez G, Alvarez J et al (2015) Fast pyrolysis of eucalyptus waste in a conical spouted bed reactor. Bioresour Technol 194:225–232. https://doi.org/10.1016/j.biortech.2015.07.030
13. Pfitzer C, Dahmen N, Troger N et al (2016) Fast pyrolysis of wheat straw in the bioliq pilot plant. Energy Fuels 30:8047–8054. https://doi.org/10.1021/acs.energyfuels.6b01412

14. Bridgwater AV (2012) Review of fast pyrolysis of biomass and product upgrading. Biomass Bioenerg 38:68–94. https://doi.org/10.1016/j.biombioe.2011.01.048
15. Funke A, Richter D, Niebel A, et al (2016) Fast pyrolysis of biomass residues in a twinscrew mixing reactor. JoVE 1–8. https://doi.org/10.3791/54395
16. Liaw S-S, Wang Z, Ndegwa P et al (2012) Effect of pyrolysis temperature on the yield and properties of bio-oils obtained from the auger pyrolysis of Douglas Fir wood. J Anal Appl Pyrolysis 93:52–62. https://doi.org/10.1016/j.jaap.2011.09.011
17. Campuzano F, Brown RC, Martínez JD (2019) Auger reactors for pyrolysis of biomass and wastes. Renew Sustain Energy Rev 102:372–409. https://doi.org/10.1016/j.rser.2018.12.014
18. Funke A, Niebel A, Richter D et al (2016) Fast pyrolysis char–assessment of alternative uses within the bioliq® concept. Bioresour Technol 200:905–913. https://doi.org/10.1016/j.biortech.2015.11.012
19. Bridgwater AV, Meier D, Radlein D (1999) An overview of fast pyrolysis of biomass. Org Geochem 30:1479–1493. https://doi.org/10.1016/S0146-6380(99)00120-5
20. Ingram L, Mohan D, Bricka M et al (2008) Pyrolysis of wood and bark in an auger reactor: physical properties and chemical analysis of the produced bio-oils. Energy Fuels 22:614–625. https://doi.org/10.1021/ef700335k
21. Oasmaa A, Kuoppala E, Gust S, Solantausta Y (2003) Fast pyrolysis of forestry residue. 1. Effect of extractives on phase separation of pyrolysis liquids. Energy Fuels 17:1–12. https://doi.org/10.1021/ef020088x
22. Burton A, Wu H (2015) Differences in bed agglomeration behavior during the fast pyrolysis of mallee bark, leaf, and wood in a fluidized-bed reactor at 500 C. Energy Fuels 29:3753–3759. https://doi.org/10.1021/acs.energyfuels.5b00651
23. Şen A, Leite C, Lima L et al (2016) Industrial valorization of Quercus cerris bark: pilot scale fractionation. Ind Crops Prod 92:42–49. https://doi.org/10.1016/j.indcrop.2016.07.044
24. Şen AU, Nobre C, Durão L et al (2022) Low-temperature biochars from cork-rich and phloem-rich wastes: fuel, leaching, and methylene blue adsorption properties. Biomass Convers Biorefinery 12:3899–3909. https://doi.org/10.1007/s13399-020-00949-x
25. Graça J, Pereira H (2000) Methanolysis of bark suberins: analysis of glycerol and acid monomers. Phytochem Anal An Int J Plant Chem Biochem Tech 11:45–51. https://doi.org/10.1002/(SICI)1099-1565(200001/02)11:1%3c45::AID-PCA481%3e3.0.CO;2-8
26. Sluiter A, Hames B, Ruiz R, et al (2008) Determination of structural carbohydrates and lignin in biomass. In: Lab. Anal. Proced. https://www.nrel.gov/docs/gen/fy13/42618.pdf. Accessed 1 Nov 2023
27. Charon N, Ponthus J, Espinat D et al (2015) Multi-technique characterization of fast pyrolysis oils. J Anal Appl Pyrolysis 116:18–26. https://doi.org/10.1016/j.jaap.2015.10.012
28. Bridgwater T (2018) Challenges and opportunities in fast pyrolysis of biomass: Part I. Johnson Matthey Technol Rev 62:118–130. https://doi.org/10.1595/205651318X696693
29. Fonseca FG, Funke A, Niebel A et al (2019) Moisture content as a design and operational parameter for fast pyrolysis. J Anal Appl Pyrolysis 139:73–86. https://doi.org/10.1016/j.jaap.2019.01.012
30. Tsai WT, Lee MK, Chang YM (2007) Fast pyrolysis of rice husk: product yields and compositions. Bioresour Technol 98:22–28. https://doi.org/10.1016/j.biortech.2005.12.005
31. Oasmaa A, Solantausta Y, Arpiainen V et al (2010) Fast pyrolysis bio-oils from wood and agricultural residues. Energy Fuels 24:1380–1388. https://doi.org/10.1021/ef901107f
32. Niebel A, Funke A, Pfitzer C et al (2021) Fast pyrolysis of wheat straw—improvements of operational stability in 10 years of Bioliq pilot plant operation. Energy Fuels 35:11333–11345. https://doi.org/10.1021/acs.energyfuels.1c00851
33. Greenhalf CE, Nowakowski DJ, Harms AB et al (2013) A comparative study of straw, perennial grasses and hardwoods in terms of fast pyrolysis products. Fuel 108:216–230. https://doi.org/10.1016/j.fuel.2013.01.075
34. Oasmaa A, Fonts I, Pelaez-Samaniego MR et al (2016) Pyrolysis oil multiphase behavior and phase stability: a review. Energy Fuels 30:6179–6200. https://doi.org/10.1021/acs.energyfuels.6b01287
35. Oasmaa A, Lehto J, Solantausta Y, Kallio S (2021) Historical review on VTT fast pyrolysis bio-oil production and upgrading. Energy Fuels 35:5683–5695. https://doi.org/10.1021/acs.energyfuels.1c00177
36. Gil L (1997) Cork powder waste: an overview. Biomass Bioenerg 13:59–61. https://doi.org/10.1016/S0961-9534(97)00033-0
37. The Board of Corticeira Amorim (2021) Sustainability Report 2020. https://amorimcorkcomposites.com/media/7331/sustainability_report_2020_en.pdf. Accessed 2 Feb 2024
38. François-Xavier Collard, Suren Wijeyekoon PB (2023) Commercial status of direct thermochemical liquefaction technologies. https://task34.ieabioenergy.com/wp-content/uploads/sites/3/2023/07/WP3.3-DTL-Final.pdf. Accessed 2 Feb 2024